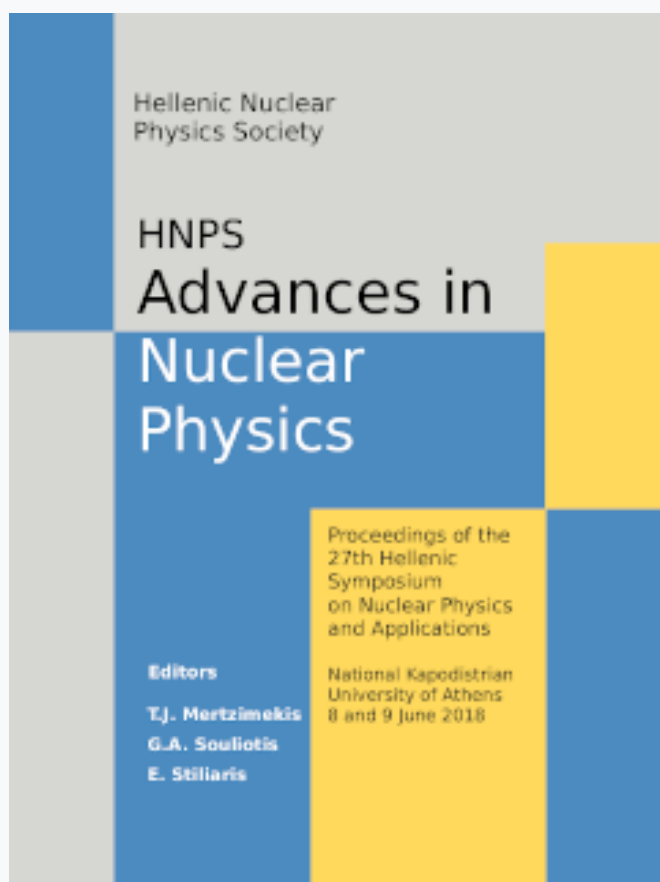


## HNPS Advances in Nuclear Physics

Vol 26 (2018)

HNPS2018



### Light flavour hadron and inclusive charged particle pT-spectra measured with the ALICE experiment at CERN

*P. Ganoti*

doi: [10.12681/hnps.1800](https://doi.org/10.12681/hnps.1800)

#### To cite this article:

Ganoti, P. (2019). Light flavour hadron and inclusive charged particle pT-spectra measured with the ALICE experiment at CERN. *HNPS Advances in Nuclear Physics*, 26, 67–74. <https://doi.org/10.12681/hnps.1800>

# Light flavour hadron and inclusive charged particle $p_T$ -spectra measured with the ALICE experiment at CERN

P. Ganoti<sup>1,\*</sup>, for the ALICE Collaboration

<sup>1</sup> *Department of Physics, Zografou Campus, National and Kapodistrian University of Athens, Greece*

---

**Abstract** Light flavor hadron and inclusive charged particle spectra provide an interesting probe of the particle production mechanisms and the transport properties of QCD matter. Charged particle and neutral meson inclusive  $p_T$ -differential cross sections in pp, p-Pb, Pb-Pb and Xe-Xe collisions have been measured by ALICE. Charged particles are studied in different multiplicity (for pp and p-Pb where available) and centrality classes (for A-A). The comparison of spectra at similar  $\langle dN_{ch}/d\eta \rangle$ , the nuclear modification factors, the mean  $p_T$  and particle ratios will also be presented considering those are observables important to get information on the properties of the medium formed in the collisions. Comparisons with model calculations will also be discussed.

**Keywords** Nuclear modification factor, neutral mesons, identified hadrons, particle ratios

---

## INTRODUCTION

Quantum chromodynamics (QCD) predicts a phase where quarks and gluons are de-confined, the quark–gluon plasma (QGP) which can be studied by colliding high energy heavy ions [1–4]. The interpretation of these results depends crucially on the comparison with those from smaller collision systems such as proton–proton (pp) or proton–nucleus (p-A).

Proton–nucleus (p-A) collisions are intermediate between proton–proton (pp) and nucleus–nucleus (A-A) collisions in terms of system size and number of produced particles. The comparison of particle production in pp, p-A, and A-A collisions has frequently been used to separate initial state effects linked to the use of nuclear beams or targets, from final state effects linked to the presence of hot and dense matter. In pp and p-A collision systems, when studying the particle production spectra as a function of the event charged multiplicity, similar features reminiscent of those already seen in A-A collisions are observed and those findings are still under investigation.

In heavy-ion collisions, transverse momentum ( $p_T$ ) spectra of charged particles and neutral mesons carry essential information about the high-density deconfined state of strongly interacting matter. For  $p_T$  up to 10 GeV/c, particle production is driven by the collective expansion of the system which is observed in the shapes of single-particle transverse-momentum spectra [5,6]. At higher  $p_T$ , particles originate from parton fragmentation and are sensitive to the amount of energy loss that the partons suffer when propagating into the medium [7]. High- $p_T$  particle suppression in heavy-ion collisions with respect to pp collisions may be modified by cold nuclear matter effects, such as nuclear parton distribution function (nPDF)

---

\* Corresponding author, email: [pganoti@phys.uoa.gr](mailto:pganoti@phys.uoa.gr)

modifications with respect to the vacuum. Measurements in p-A collisions are thus needed to disentangle cold nuclear effects from the observed high- $p_T$  particle production suppression in AA collisions.

The modification of hadron yields in A-A collisions with respect to pp collisions is quantified by the nuclear modification factor,  $R_{AA}$  which is expressed as follows:

$$R_{AA} = \frac{dN_{AA}/dp_T}{\langle N_{coll} \rangle \times dN_{pp}/dp_T} = \frac{dN_{AA}/dp_T}{\langle T_{AA} \rangle \times d\sigma_{pp}/dp_T}$$

where  $N_{AA}$  and  $N_{pp}$  are the particle yields in A-A and pp collisions, respectively and  $\sigma_{pp}$  is the production cross section in pp collisions. The nuclear overlap function  $\langle T_{AA} \rangle = \langle N_{coll} \rangle / \sigma_{pp,INEL}$  is related to the average number of inelastic nucleon-nucleon collisions. In the factorization approach of a perturbative QCD calculation of particle production from hard scattering, the overlap function  $T_{AA}$  can be interpreted as the increase of the parton flux going from pp to A-A collisions. Without nuclear effects,  $R_{AA}$  will be consistent with unity in the hard scattering regime [8].

In the next sections, selected results from neutral mesons and charged particles will be presented and discussed.

## RESULTS FROM NEUTRAL MESONS

Neutral mesons ( $\pi^0$  and  $\eta$ ) are reconstructed in ALICE [9] via the invariant mass technique by using four different detectors: the electromagnetic calorimeters PHOS [10] and EMCal [11] and the two tracking detectors, the Inner Tracking System [12] (ITS) and the Time Projection Chamber [13] (TPC). In the calorimeters, the electron and photon reconstruction is made by measuring the electromagnetic showers produced by the incident particles. The two tracking devices are used to reconstruct tracks and the electrons and positrons identification is performed by measuring the energy loss in the TPC. After their identification, electrons and positrons are paired to reconstruct conversion photons. This is the Photon Conversion Method (PCM). The three systems (EMCal, PCM and PHOS) are complementary, they contribute in different  $p_T$  ranges of the neutral meson spectra but there are also overlapping regions.

$\pi^0$  and  $\eta$  spectra have been measured from 0.3-0.4 GeV/c up to 30-40 GeV/c depending on the particle type, the method and the system, in pp, p-Pb and Pb-Pb at different center-of-mass energies, from which the nuclear modification factors are calculated. In figure 1, the nuclear modification factors  $R_{pPb}$  are shown for both  $\pi^0$  and  $\eta$  [14]. Both factors are consistent with unity above 2 GeV/c implying the absence of nuclear effects in this  $p_T$  region.

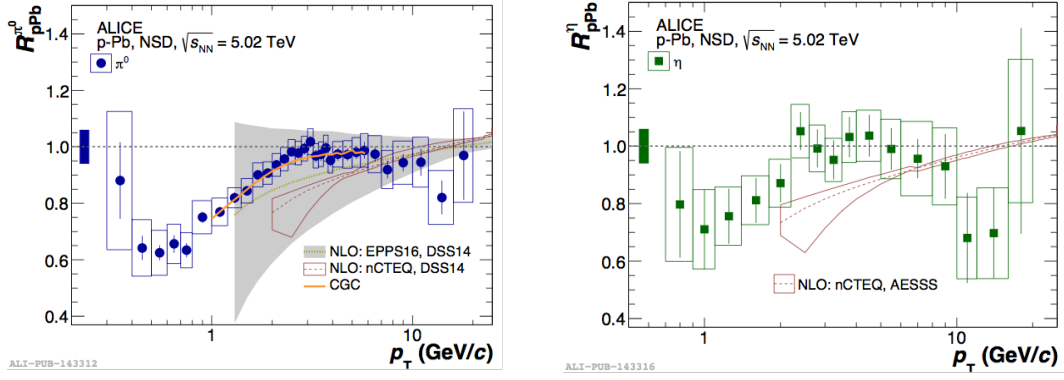


**Fig. 1.** Nuclear modification factors  $R_{pPb}$ , for  $\pi^0$  (left) and  $\eta$  (right) mesons measured in NSD p-Pb collisions at centre-of-mass energy 5.02 TeV. pQCD calculations at NLO with different parton distribution functions (PDFs) and fragmentation functions (FFs) are also plotted. Color Glass Condensate predictions using the  $k_T$  factorization are shown for  $\pi^0$ .

The analysis of pp and Pb-Pb [15-17] collisions at center-of-mass energies 2.76 TeV and 5.02 TeV allows the calculation of the nuclear modification factor  $R_{AA}$  in different centrality bins and the comparison between the two energies (figure 2). From this figure, the conclusion is that  $R_{AA}$  is centrality dependent but not energy dependent. The observed suppression is due to the parton energy loss in the hot and dense medium created in heavy-ion collisions.

## RESULTS FROM CHARGED PARTICLES

The study of identified charged particles, as baryons and mesons, is of fundamental interest because of the differences in the dynamics of fragmentation between quarks and gluons to baryons and mesons [18], and furthermore because they allow to study the differences in their interaction with the medium considering that due to the color Casimir factor, gluons lose a factor of two more energy than quarks [19, 20].

Light charged hadrons (pions, kaons and protons) are identified over a wide transverse momentum range, from few hundred MeV/c to several GeV/c depending on the particle and the analysis method, by measuring their energy loss  $dE/dx$  in ITS and TPC detectors and the time-of-flight in the TOF detector. Kaons can also be identified by using their topological weak decays to muons and muon neutrinos ( $K^\pm \rightarrow \mu^\pm + \nu_\mu$ ).

Pion, kaon and proton spectra have been studied in all available collision systems, pp, p-Pb, Pb-Pb and Xe-Xe at various energies as a function of centrality for heavy-ions or as a function of multiplicity for the lighter systems such as pp and p-Pb.

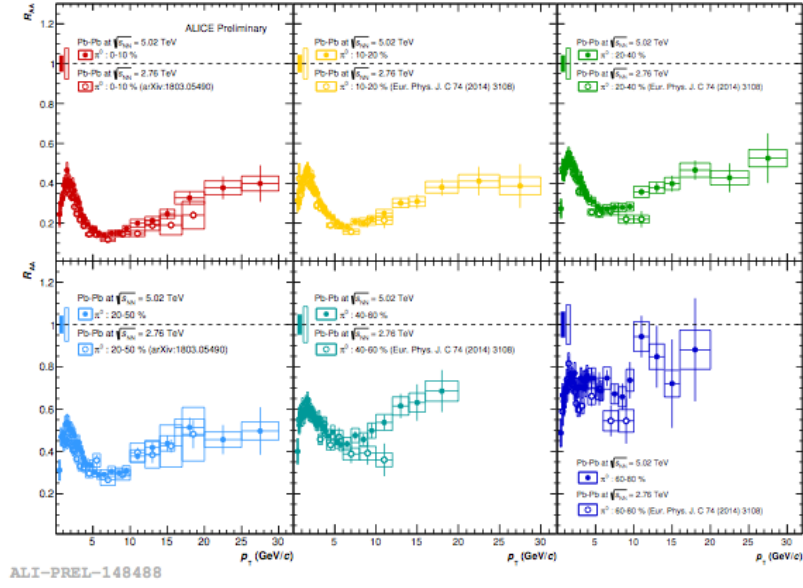


**Fig. 2.**  $\pi^0$  nuclear modification factors ( $R_{AA}$ ), in different bins of centrality and for centre-of-mass energies 2.76 TeV and 5.02 TeV.

In figure 3, the pion ( $\pi^+\pi^-$ ), kaon ( $K^+K^-$ ) and proton ( $p+p$ ) spectra in pp collisions at center-of-mass energy 13 TeV are shown as a function of the event charged particle multiplicity.

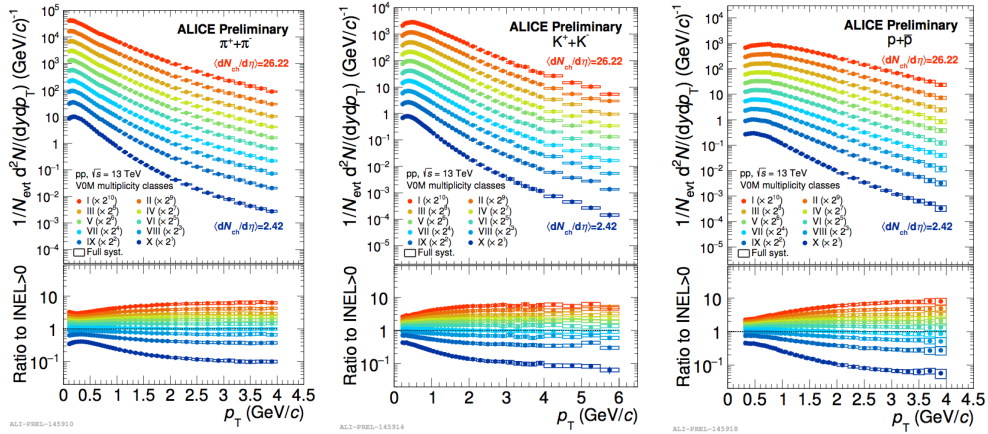


**Fig. 3.** Pion, kaon and proton spectra in pp collisions at centre-of-mass energy 13 TeV as a function of the event multiplicity. The bottom plots show the ratio of the spectra to the INEL>0 event class.

In figure 4, the same spectra in Pb-Pb collisions at center-of-mass energy 5.02 TeV are presented as a function of centrality, which can be translated to the charged particle multiplicity. In this way, a direct comparison of pp collisions with heavy-ion collisions is possible at similar multiplicities.

A similar evolution of the production of the three particles with multiplicity is observed in both pp and Pb-Pb collisions. Such results provide useful information on the system

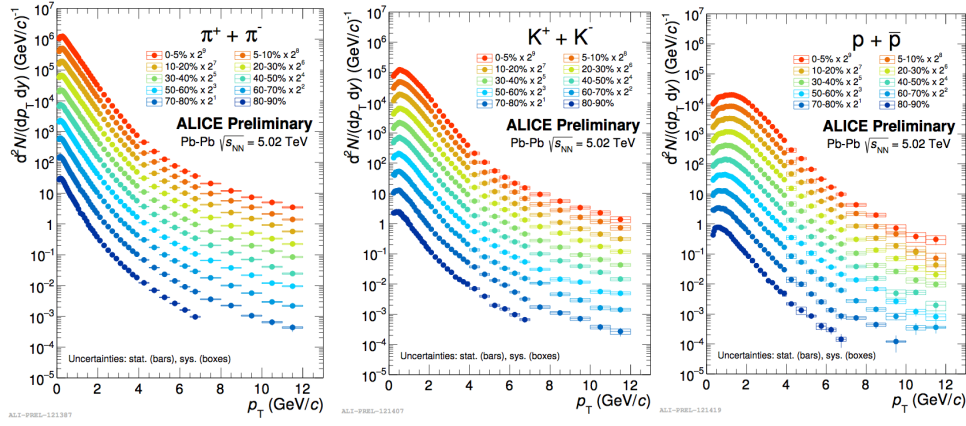


**Fig. 4** Pion, kaon and proton spectra in Pb-Pb collisions at centre-of-mass energy 5.02 TeV as a function of centrality.

chemistry and dynamics and help in testing hydrodynamic models.

In figure 5, the  $p_T$ -integrated  $K/\pi$  and  $p/\pi$  ratios as a function of the charged particle multiplicity at various center-of-mass energies in pp, p-Pb and Pb-Pb collisions are presented.

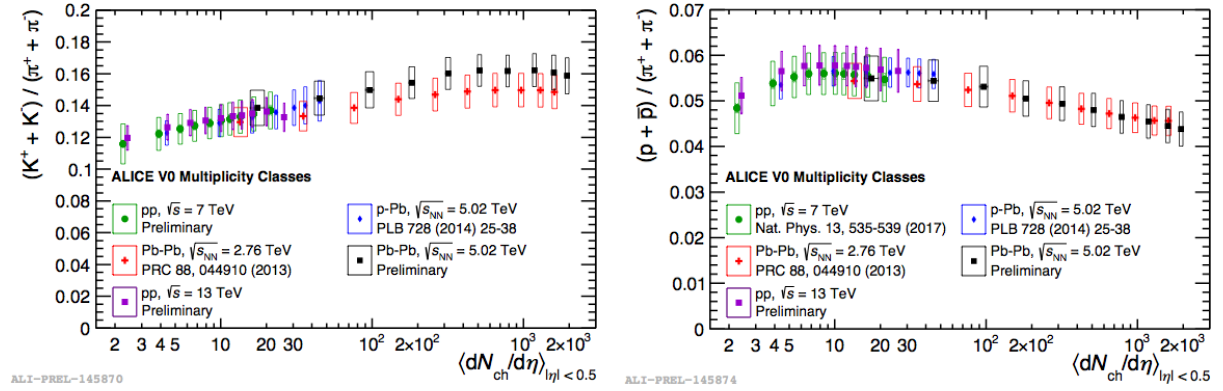


**Fig. 5.**  $p_T$ -integrated  $K/\pi$  and  $p/\pi$  ratios as a function of the charged particle multiplicity in pp, p-Pb and Pb-Pb collisions at different energies. Bars and boxes represent statistical and systematic uncertainties, respectively.

The particle ratios within their uncertainties seem to depend only from the charged particle multiplicity regardless the type of collision and the energy, thus suggesting that the particle chemistry is driven by the multiplicity. Figure 6, confirms this result, where the  $p_T$  dependence of the  $p/\pi$  ratio is compared for two heavy-ion systems, Pb-Pb and Xe-Xe at similar multiplicities.

A very interesting feature is revealing from the comparison of the same property in different multiplicity classes and for different collision systems, starting from the lightest pp systems to the heavier Pb-Pb ones (figure 7). For Pb-Pb collisions, it was known that the  $p_T$

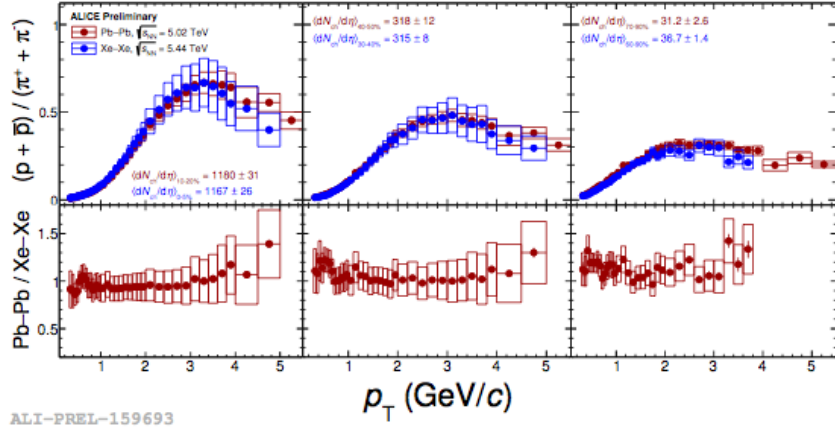


**Fig. 6.**  $p/\pi$  ratios as a function of  $p_T$  in Pb-Pb and Xe-Xe collisions at similar charged particle multiplicities and their ratios.

where the baryon-to-meson ratios become maximum exhibits a blueshift going from low to high multiplicity events and a similar behavior is observed in lighter systems like pp and p-Pb [21]. For Pb-Pb the effect is reproduced by models, incorporating hydrodynamic expansion and parton recombination, however, there is still no unique explanation.

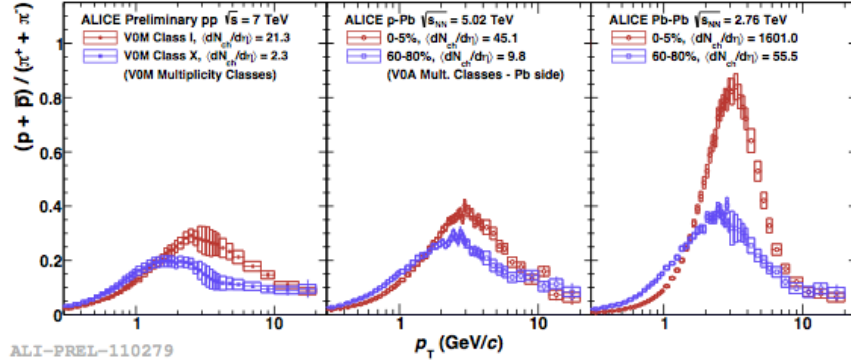


**Fig. 7.**  $p/\pi$  ratios as a function of  $p_T$  and in different multiplicity classes for pp, p-Pb and Pb-Pb collisions.

The transverse momentum spectra of the measured hadrons become harder with increasing centrality. This results from figure 8, where the average transverse momentum,  $\langle p_T \rangle$ , is plotted as a function of centrality for charged particles in heavy-ion collisions (left) [22] and as a function of multiplicity for identified pions, kaons and protons in pp collisions (right). The  $\langle p_T \rangle$  of identified hadrons follows mass ordering and seems to depend on the charged particle multiplicity and not on the center-of-mass energy. These observations are consistent with expectations from hydrodynamics, as particles in the expanding system experience the same radial velocity field [23].

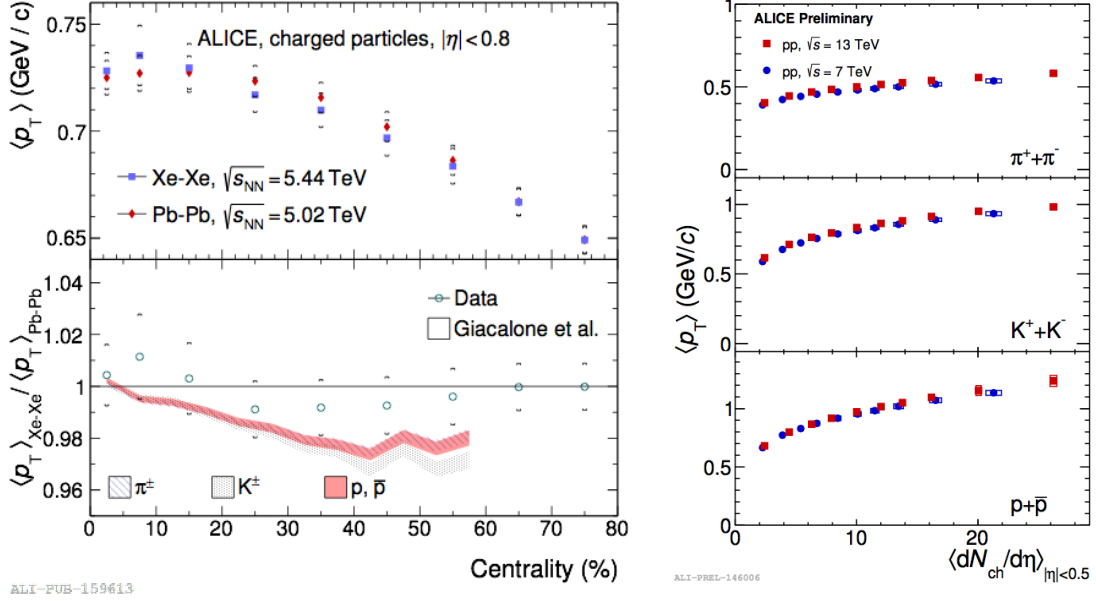


**Fig. 8.** Left: Centrality dependence of the average transverse momentum of charged particles in Xe–Xe and Pb–Pb collisions and their ratio. The hashed area in the ratio is the result from hydrodynamical calculations for pions, kaons and protons. Right: Multiplicity dependence of the average transverse momentum for pions, kaons and protons in pp collisions at centre-of-mass energies 7 and 13 TeV.

The Boltzmann-Gibbs blast-wave model [24] (a simplified hydrodynamic model) is used in order to extract the kinetic freeze-out temperature,  $T_{\text{kin}}$ , and the radial expansion velocity,  $\beta_T$ , of the system [25] by performing a simultaneous fit to the  $p_T$  spectra of pions, kaons and protons. Figure 9 shows the correlation between these two variables for different collision systems at different collision energies as a function of the charged multiplicity. Charged multiplicity increases from left to right, thus  $\beta_T$  is increasing with multiplicity. The kinetic freeze-out temperature is higher in small systems for the same charged multiplicity. This picture is in agreement with the conclusion that the evolution of a colliding system seems to depend only on the charged multiplicity, regardless the type of the colliding nucleus.

## CONCLUSIONS

Results on neutral mesons and charged particles measured by ALICE have been presented. These results are obtained from observables calculated starting from the  $p_T$  spectra of the particles such as nuclear modification factors, mean  $p_T$  and particle ratios. By combining measurements from different systems and comparing with models we gain insights into the features of the medium formed in the various collisions and the particle production mechanisms.

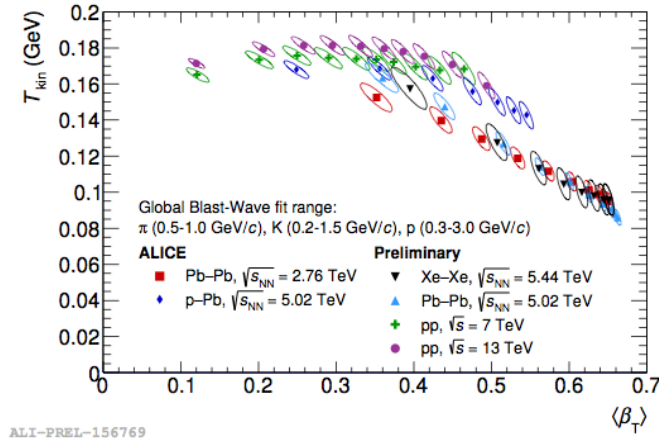


**Fig. 9.** The kinetic freeze-out temperature,  $T_{\text{kin}}$ , and the radial expansion velocity,  $\beta_T$ , for different collision systems and energies, for different charged multiplicities as calculated from the Boltzmann-Gibbs blast-wave model.

There is a continuous evolution with multiplicity of the observables mentioned above. The analysis of all available data and the detailed comparisons with theoretical models will provide a better understanding.

## References

- [1] N. Cabibbo, G. Parisi, Phys.Lett. B 59, 67 (1975)
- [2] E.V. Shuryak, Phys. Lett. B 78, 150 (1978)
- [3] L.D. McLerran, B. Svetitsky, Phys. Lett. B 98, 195 (1981)
- [4] E. Laermann, O. Philipsen, Ann. Rev. Nucl. Part. Sci. 53, 163 (2003)
- [5] ALICE Collaboration, J. Adam et al, Phys. Rev. C 93, 024917 (2016)
- [6] ALICE Collaboration, S. Acharya et al., arXiv 1802.09145 (2018)
- [7] J. Bjorken, Tech. Rep. FERMILAB-PUB-82-059-T, Fermilab (1982)
- [8] X.-N. Wang and M. Gyulassy, Phys. Rev. Lett. 68, 1480 (1992)
- [9] K. Aamodt et al., JINST 3, S08002 (2008)
- [10] ALICE Collaboration, Technical design report of Photon Spectrometer, CERN/ LHCC99-4
- [11] ALICE Collaboration, Technical design report of the ALICE Electromagnetic Calorimeter, CERN/ LHCC-2008-014 (2008)
- [12] K. Aamodt et al., JINST 5, P03003 (2010)
- [13] J. Alme et al., Nucl. Instrum. Meth. A 622, 316 (2010)
- [14] ALICE Collaboration (Shreyasi Acharya et al.), Eur. Phys. J. C 78, 624 (2018)
- [15] ALICE Collaboration (Shreyasi Acharya et al.), arXiv:1803.05490 (2018)
- [16] ALICE Collaboration (Shreyasi Acharya et al.), Eur. Phys. J. C 77, 339 (2017)
- [17] ALICE Collaboration (Betty Bezverkhny Abelev et al.), Eur. Phys. J. C 74, 3108 (2014)
- [18] P. Abreu, et al., Eur. Phys. J. C 17, 207 (2000)
- [19] X.-N. Wan, Phys. Rev. C 58, 2321 (1998)
- [20] T. Renk, K.J. Eskola, Phys. Rev. C 76, 041902 (2007)
- [21] S. Acharya et al. (ALICE Collaboration), arXiv:1807.11321
- [22] S. Acharya et al. (ALICE Collaboration), arXiv:1805.04399
- [23] Francesca Bellini (for the ALICE Collaboration), arXiv:1808.05823
- [24] E. Schnedermann, J. Sollfrank, U.W. Heinz, Phys. Rev. C 48, 2462 (1993)
- [25] B. Abelev et al. (ALICE Collaboration), Phys. Rev. C 88, 044910 (2013)